Autophagy-inducing peptides from mammalian VSV and fish VHSV rhabdoviral G glycoproteins (G) as models for the development of new therapeutic molecules

Pablo García-Valtanen,[1,†] María del Mar Ortega-Villaizán,[1,†] Alicia Martínez-López,[1] Regla Medina-Gali,[2] Luis Pérez,[1] Simon Mackenzie,[3] Antonio Figueras,[4] Julio M Coll,[5] and Amparo Estepa[1,*]

[1]IBMC; Miguel Hernández University; Elche, Spain; [2]Labiofam; La Habana, Cuba; [3]Institute of Aquaculture; University of Stirling; Stirling, UK; [4]Instituto de Investigaciones Marinas (IIM); CSIC; Vigo, Spain; [5]INIA-SIGT–Biotecnología; Madrid, Spain

[†]These authors contributed equally to this work.

It has not been elucidated whether or not autophagy is induced by rhabdoviral G glycoproteins (G) in vertebrate organisms for which rhabdovirus infection is lethal. Our work provides the first evidence that both mammalian (vesicular stomatitis virus, VSV) and fish (viral hemorrhagic septicemia virus, VHSV, and spring viremia carp virus, SVCV) rhabdoviral Gs induce an autophagic antiviral program in vertebrate cell lines. The transcriptomic profiles obtained from zebrafish genetically immunized with either Gsvcv or Gvhsv suggest that autophagy is induced shortly after immunization and therefore, it may be an important component of the strong antiviral immune responses elicited by these viral proteins. Pepscan mapping of autophagy-inducing linear determinants of Gvhsv and Gvsv showed that peptides located in their fusion domains induce autophagy. Altogether these results suggest that strategies aimed at modulating autophagy could be used for the prevention and treatment of rhabdoviral infections such as rabies, which causes thousands of human deaths every year.

Introduction

Macroautophagy, or simply autophagy, refers to a nonspecific degradation processes by which cells deliver cytoplasmic substrates to lysosomes for their degradation.[1-3] Autophagy is an evolutionarily conserved membrane-trafficking process that operates at low basal levels under normal conditions and maintains the cellular metabolic balance and homeostasis. Besides its role in healthy catabolic processes, autophagy is an important component of the host response against infectious agents. For instance, autophagy mediates both surveillance and effector functions involved in the detection and clearance of viruses.[4,5] Thus, strategies aimed at modulating autophagy could be used in the prevention and treatment of infectious diseases.

The first description of autophagy-like structures in virus-infected cells was made by Palade et al. who visualized poliovirus particles inside cell vacuoles similar to autophagosomes.[6] Despite this early observation, the significance of autophagy in virus infections remained elusive until recent years.[7] Today, it is known that autophagy can play either antiviral or proviral roles during viral infection, depending on the virus. For example, the herpes simplex virus-1 triggers autophagy[8] leading to its degradation in host cells[9,10] whereas polioviruses[11] or dengue virus[12,13] use autophagy to favor their replication.

The role(s) played by autophagy in rhabdovirus pathogenesis is not fully described yet. In the model organism *Drosophila*, autophagy inhibits both in vitro and in vivo the replication of the mammalian rhabdovirus VSV (vesicular stomatitis virus).[14] Furthermore, the glycoprotein G of VSV appears to be the pathogen-associated molecular pattern (PAMP) that, after interacting with *Toll-7* (toll receptor 7), activates the autophagic antiviral program.[14-16] Whether or not the glycoprotein G plays a similar

role in rhabdovirus vertebrate host organisms for which rhabdoviral infection is lethal remains unexplored.

Here we show, for the first time, that autophagy inhibits fish rhabdovirus replication. In addition, the glycoprotein G (G) of 3 different viruses, a mammalian rhabdovirus (VSV), and 2 fish rhabdoviruses (viral hemorrhagic septicemia virus, VHSV, and spring viremia of carp virus, SVCV) were used to study both in vitro and in vivo their potential to induce autophagy in the model vertebrate species zebrafish (*Danio rerio*). Our results show that VSV, VHSV, and SVCV Gs, in the absence of other viral components, are sufficient to induce a cell's antiviral autophagic program in vitro. Transcriptomic analysis from genetically immunized zebrafish as well as in vitro gene expression assays suggest that autophagy might contribute strongly to the immune responses induced by mammalian and fish rhabdoviral Gs. Moreover, the linear regions of rhabdoviral Gs involved in inducing autophagy were identified in accordance to their ability to induce autophagy and control rhabdovirus infection in vitro. Since immunization strategies to prevent and/or control rhabdoviral infections might benefit from the use of molecules that promote autophagy to degrade virus particles or improve their recognition, this study opens the door for the development of a new class of antiviral drugs/viral vaccine adjuvants. At the same time, this study also highlights the importance of increasing the knowledge on host and cellular barriers against virus infection (e.g., autophagy) to find new therapeutic targets.

Results

Fish rhabdoviruses induce antiviral autophagy

To test whether or not fish rhabdoviruses induce autophagy, ZF4 cells were infected with VHSV or SVCV. The aggregation (puncta formation) of endogenous MAP1LC3A/B (microtubule-associated protein 1 light chain 3, α/β, described as LC3 henceforth), 2 mammalian orthologs of yeast Atg8, which is directly implicated in the membrane-elongation step of autophagosomes[17]) was assayed 24 h later by IF using an anti-LC3 antibody. Increased LC3 puncta was observed in both VHSV- and SVCV-infected ZF4 cells compared with uninfected cells (**Fig. 1A**). A similar fluorescence expression pattern was observed after treating ZF4 cells with rapamycin (rapamycin induces autophagy by inhibiting MTOR [mechanistic target of rapamycin]) (**Fig. S1**).

To check whether replication of SVCV or VHSV was inhibited by autophagy, as is the case for VSV,[14] 3-methyladenine (3MA)-treated cells (3MA inhibits autophagy by blocking the formation of autophagosomes) were infected with VHSV or SVCV and the amount of viral particles released after 24 h into the cell culture media was titrated. Treatment of cells with 3MA prior to infection reduced > 2-fold the SVCV or VHSV yield from infected cells compared with cell cultures without 3MA treatment (**Fig. 1B**) indicating that autophagy can inhibit fish rhabdovirus replication. These results confirm previous reports describing the effect of autophagy activation upon VSV replication,[14] suggesting that

this might be a trait common to members of the *Rhabdoviridae* family.

On the other hand, no effects of 3MA or rapamycin on the cell viability were observed (not shown).

Activation of authophagy by VSV, VHSV, and SVCV Gs

The implication of other rhabdoviral Gs in the activation of antiviral autophagy has been demonstrated in assays using UV-inactivated VSV infection and Gvsv-containing vesicular particles in *Drosophila*,[14,15] an invertebrate model species. However, antiviral autophagy induction by rhabdoviral Gs in vertebrates has not been tested. This might be an important difference since, in contrast to VSV infections in *Drosophila*, rhabdoviral infections in vertebrates are often lethal. To that end, plasmid constructs containing the cDNA sequence coding for the VSV, VHSV, or SVCV Gs, fused to the sequence encoding the teal fluorescent protein (TFP)[18] were obtained and used to transfect the fish cell line ZF4 (Gsvcv and Gvhsv) and the mammalian cell line HaCaT (Gvsv). Cells transfected with pmTFP (encoding monomeric TFP) showed fluorescence diffusely distributed in the cytoplasm and the nucleus in both ZF4 and HaCaT cells (**Fig. 2**). In contrast, cells transfected with the plasmids encoding the G-TFP fusion proteins showed a relocalization of the fluorescence in both cell lines. The majority of these cells exhibited a nonuniform granulated cytoplasmic and plasma membrane distribution of the fluorescence and the fluorescence was excluded from the nuclear region (**Fig. 2**). No effects of the G expression upon cell morphology or viability were observed (not shown).

On the other hand, to investigate whether or not zebrafish cells might be a good model for studies implicating the G of the mammalian rhabdovirus VSV, ZF4 cells were also transfected with pGvsv-TFP. Results showed fluorescence indicative of a normal level of expression of the G protein (**Fig. 2**).

Likewise, functionality of the 3 fusion proteins seemed correct in cell culture as indicated by low-pH dependent fusion assays (**Fig. S2**). G-induced autophagy was then evaluated (**Fig. 3**). An increased number of cells showing fluorescent cytoplasmic puncta representing LC3-containing autophagosomes was observed in both the ZF4 and HaCaT cells transfected with G-TFP fusion proteins (**Fig. 3A**) compared with both untransfected (not shown) and pm-TFP-transfected cells (**Fig. S3A and S3C**). Similar results were obtained after transfection of ZF4 cells with pGvsv-TFP (**Fig. S3B**). Increased autophagy was also observed in the cells surrounding G-TFP-transfected cells (**Fig. 3A**).

In mammals, after autophagy induction, the cytosolic form of LC3 (LC3-I) is conjugated on its carboxyl terminus with phosphatidylethanolamine forming the lipidated phagophore (autophagosome precursor)/autophagosomal membrane-bound form of LC3 (LC3-II). A portion of this LC3-II remains on the mature autophagosome. Therefore, the amount of LC3-II correlates with the number of autophagosomes and it constitutes the recognized consensus marker of this structure. Since anti-LC3 antibodies recognize both LC3-I and LC3-II, autophagy progression can be also monitored by immunoblotting assays[14,19] and quantified by calculating the LC3-II/LC3-I ratio. The LC3-II/LC3-I ratios (**Fig. 3B**) in rhabdoviral G-transfected cells (4.92, 4.51 and 2.05
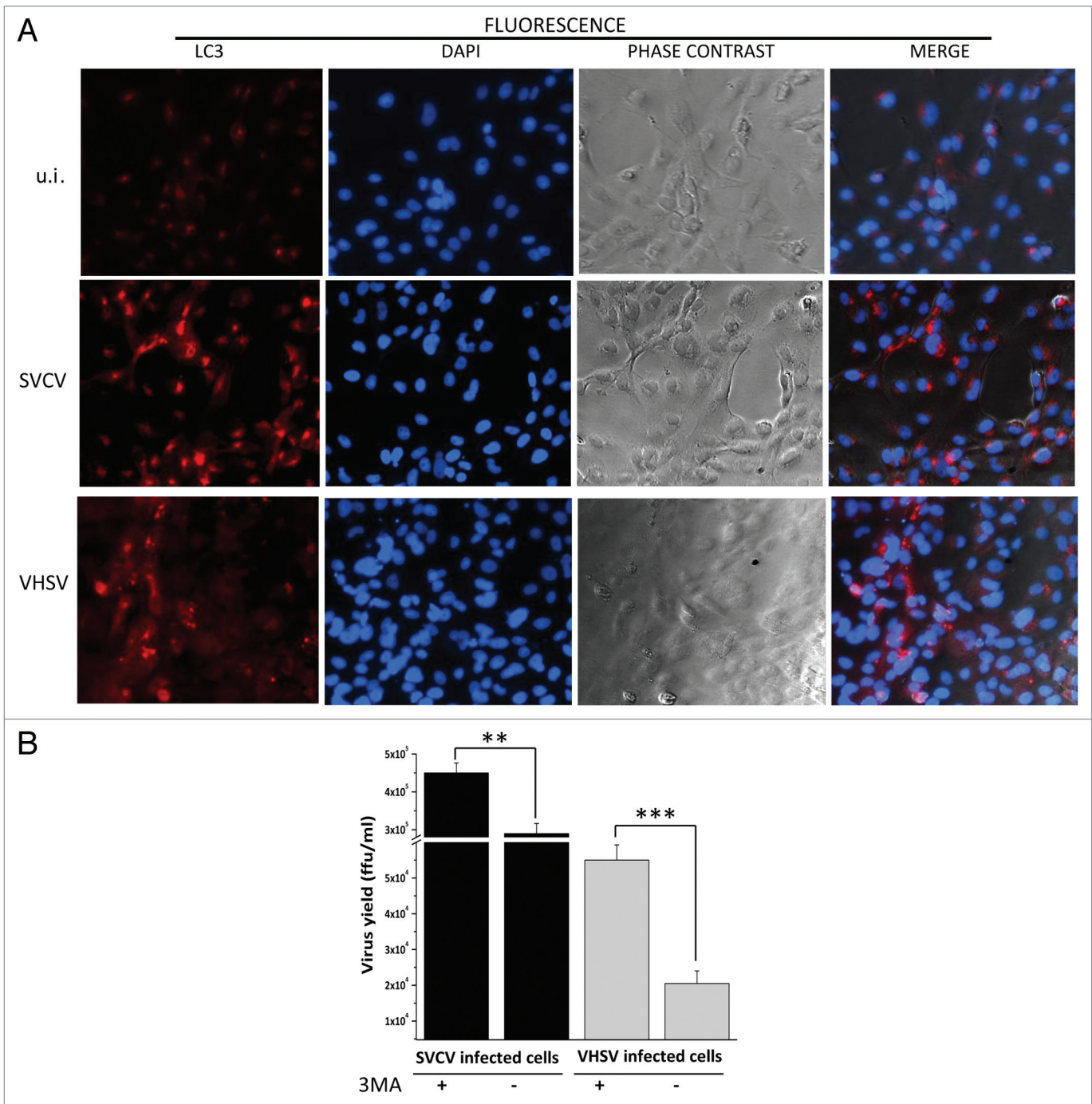
Figure 1. Autophagy after fish rhabdoviral infection and its antiviral effect in zebrafish cells. (**A**) ZF4 cells were infected with either SVCV or VHSV (moi = 1) or uninfected (u.i.) and fixed after 24 h. Cells were then incubated with an antibody anti-LC3 and stained with a fluorophore-conjugated secondary antibody (red fluorescence, LC3), and DAPI (blue, cell nuclei). Images are representative of the results obtained in 2 independent experiments (**B**) Titration in EPC cells of virus in ffu/mL recovered from cell culture media of ZF4 cells with or without 3MA (10 mM) pretreatment and then infected with either SVCV (black bars) or VHSV (gray bars) (both at moi = 2). Results represent the mean ± SD of 2 independent experiments each performed in duplicate. ** and ***, Statistically significant ($P \leq 0.05$ and $P \leq 0.01$, respectively).

for SVCV, VHSV, and VSV G-transfected cells, respectively) were ~2-fold higher than in TFP-transfected (1.64 and 0.92 for ZF4 and HaCaT cells, respectively) or control cells (1.47 and 0.23 for ZF4 and HaCaT cells, respectively). These results clearly indicate that the conversion of LC3-I to LC3-II was promoted in both fish and mammalian cells by the viral glycoproteins after transfection. In ZF4 cells the LC3-II/LC3-I ratios were similar in G-transfected and UV-inactivated virus infected cells (4.32 and 4.19 for VHSV-UV and SVCV-UV, respectively). As expected, cells infected with live virus (11.04 and 11.64 for SVCV- and
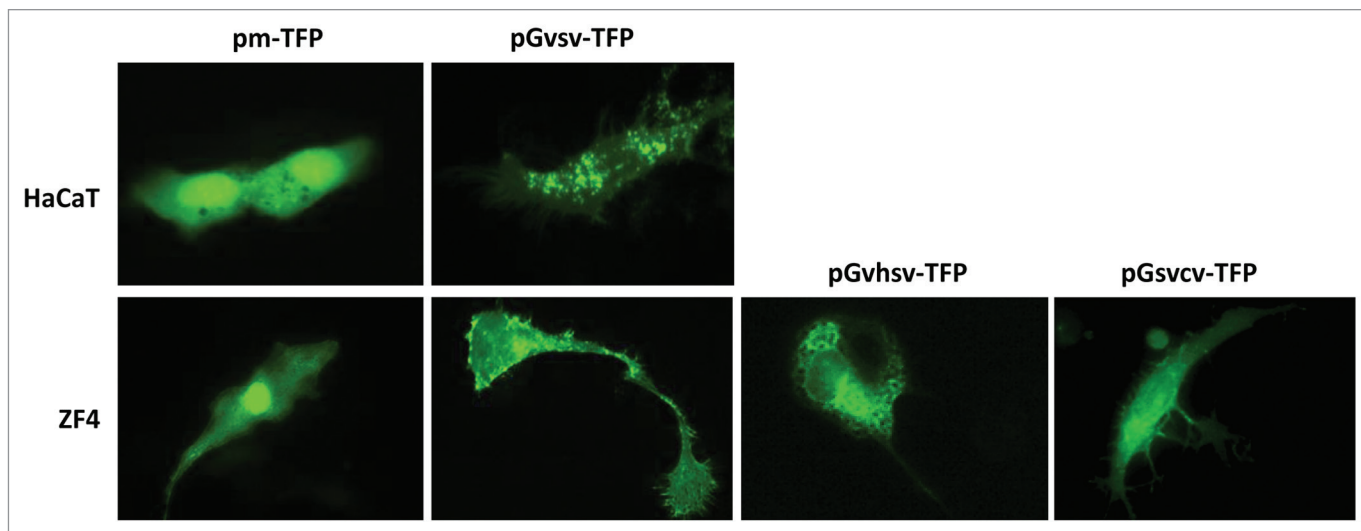
Figure 2. Expression of G-TFP fusion proteins in fish and mammalian cells. HaCaT or ZF4 cells were transfected with 1 μg/mL of pmTFP, pGvsv-TFP, pGvhsv-TFP, or pGsvcv-TFP and then viewed and photographed with an inverted fluorescence microscope 48 h post-transfection.

VHSV-infected cells, respectively) or treated with rapamycin (11.06) showed the highest LC3-II/LC3-I ratios (**Fig. 3B**). All together, these experiments demonstrate that i) fluorescent puncta are autophagosomes and ii) rhabdoviral Gs are inducing autophagosome (LC3-II) formation.

Rhabdoviral Gs also induce autophagy in in-vivo transfected cells

An important question is whether the autophagy induced by rhabdoviral Gs in vitro extends to in vivo conditions. If this is the case, autophagy should be detected at short times post-immunization with G. To investigate this aspect and in order to keep a certain degree of similitude between both in vitro (cell transfection) and in vivo experiments, adult zebrafish were genetically immunized by intramuscular injection with the G-encoding plasmids (in vivo cell transfection). Three ds after immunization, muscle samples at the site of injection were taken and processed for a gene expression study. Glycoproteins of VHSV and SVCV were chosen for the in vivo assays because DNA vaccines based on these glycoproteins, when intramuscularly injected, conferred fish protection against virus lethal challenges.[20-23]

First, since the in vivo conditions governing the expression of the proteins encoded by the plasmids might be different from those in vitro,[24] their expression in the muscle (i.e., injection site) was assessed by RTqPCR. Expression of both Gs was observed (**Fig. S4**). However, the relative amount of transcripts of the Gs (expression values normalized against *eef1a1l1* [eukaryotic translation elongation factor 1 α, like 1] expression) varied from fish to fish, although the average expression levels of both Gs were similar (**Fig. S4**).

To investigate how the genes implicated in autophagy are regulated in response to immunization with the G-encoding plasmids, analysis of the whole-transcriptome profiles rather than measurement of the expression of several potential candidate autophagy related-genes were performed. Thus, we conducted a transcriptome analysis from: pAE6-Gvhsv-, pAE6-Gsvcv-, pAE6-injected and uninjected (control [C]) zebrafish groups.

Both of the transcriptomic profiles of zebrafish intramuscularly injected with G-encoding plasmids (pAE6-Gsvcv or pAE6-Gvhsv) showed significant modulation of autophagy-associated genes. One hundred 50 genes (**Table S2**) out of 420 identified in mammals as participants of autophagy and autophagy-related processes (including genes of the lysosomal pathway),[25] and present in the microarray used for these experiments, were commonly modulated by both pAE6-Gsvcv and pAE6-Gvhsv. The results confirm that autophagy-related genes are involved in the orchestration of the host immune response to these viral antigens. According to Jegga et al.,[25] those 150 genes are classified in *autophagy*, and are involved in autophagosome formation (9% of the G-modulated genes), *autophagy regulators* (45%), *lysosomal function* (17%) and *lysosomal regulator* (29%) genes (**Fig. 4A**).

The modulation of genes classified as *autophagy* genes (13 genes, **Fig. 4B**) suggests that autophagy takes place in vivo in response to G expression. Moreover, these genes encode molecules implicated in several stages of the autophagosome biogenesis. For instance, *ulk1* (*ULK1* in humans and *Ulk1* in mice, a mammalian ortholog of yeast *ATG1*) encodes a protein kinase in yeast and mammals,[26-29] which regulates formation of phagophores. The genes encoding Atg4 isoforms (*atg4b* and *atg4c*, **Fig. 4B**), encode cysteine proteases that cleave the C-terminal amino acids of LC3 in order to allow LC3 conjugation with phosphatidylethanolamine.[30,31] The *atg5* and *atg12* genes encode proteins that are part of a complex. In mammals, this complex formed by ATG12, ATG5, and ATG16L1 is necessary for the lipidation of LC3 and the elongation of the phagophore.[32] On the other hand, ATG7 and ATG10 enable the union between ATG12 and ATG5.[32] The *becn1* gene (*BECN1* in humans, *Becn1* in mice or *VPS30/ATG6* in yeast) encodes Becn1 in zebrafish or BECN1 in mammals, a key protein molecule in the class III phosphatidylinositol 3-kinase (PtdIns3K) complex, crucial in autophagosome formation in
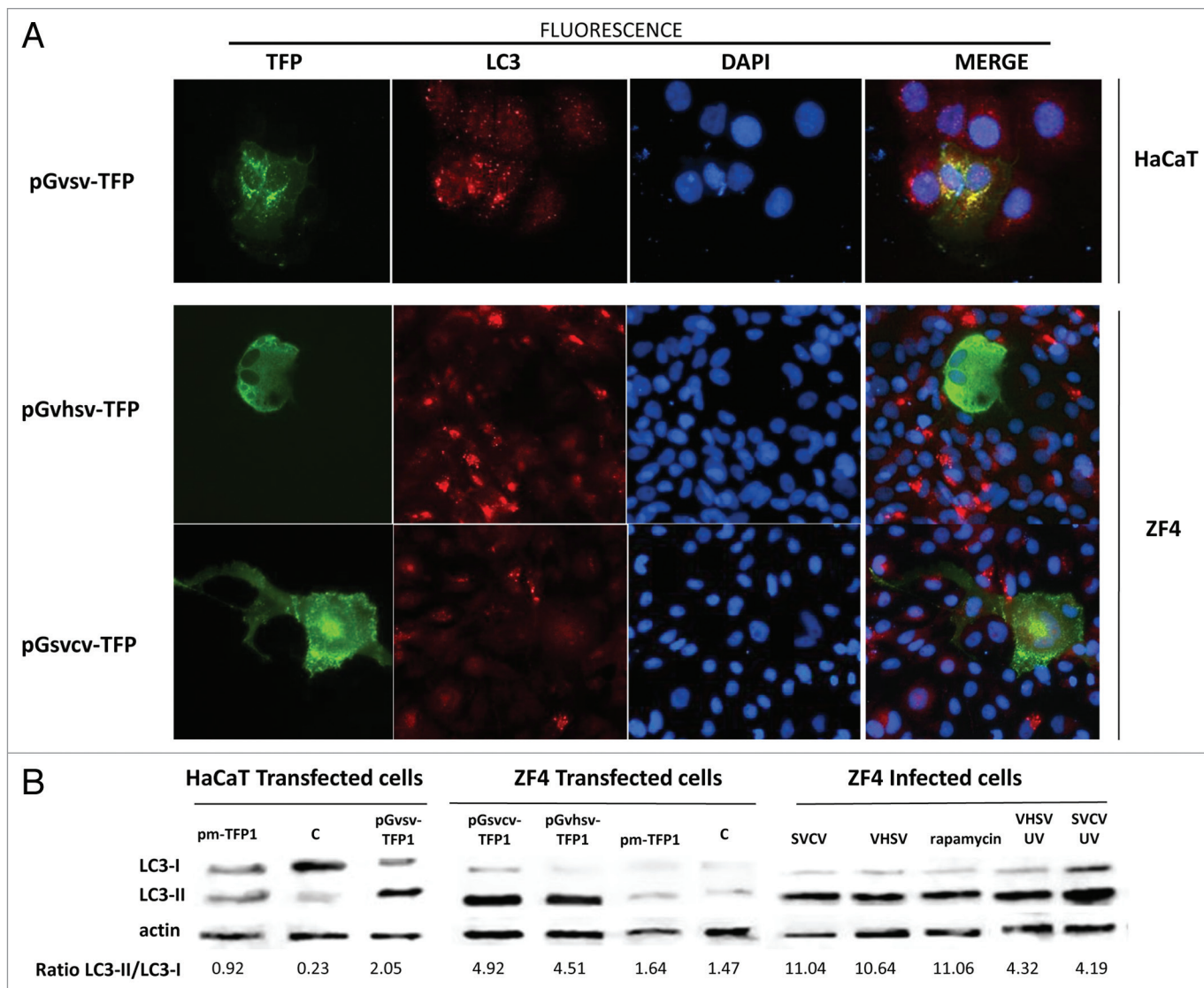
Figure 3. Rhabdoviral G-mediated autophagy in cells transfected with pm-TFP, pGvsv-TFP, pGvhsv-TFP or pGsvcv-TFP (**A**) and LC3-II/LC3-I ratios in virus infected and G-transfected cells. (**A**), cells were fixed at 72 h after transfection with 2.5 μg/mL of pGvsv-TFP (HaCaT cells) or 0.5 μg/mL of either pGvhsv-TFP or pGsvcv-TFP (ZF4 cells), for LC3 staining with an antibody anti-LC3 and fluorescent visualization. (**B**) Whole cell lysates were obtained from cells transfected (as above) or infected with SVCV, VHSV, or UV irradiated viruses (SVCV-UV, VHSV-UV) at moi = 20 for 4 h, cells treated with 500 nM of rapamycin (4 h) or untreated cells (control, C). LC3-I and LC3-II bands were visualized by WB using an anti-LC3 antibody, and the protein content of the stained bands estimated by densitometry, densitometry values were used to calculate LC3-II/ LC3-I ratios. Additionally, as a protein load internal control, actin bands were visualized using an anti-actin antibody. Results are representative of 2 independent experiments.

yeast and mammals.[32] The role of the mammalian homologs of the zebrafish Wipi1 protein, also upregulated in zebrafish cells upon G expression (**Fig. 4B**), remains to be completely elucidated.[32] Interestingly, WIPI1 plays a role in xenophagic processes against bacteria in human cells.[33] The *lc3a* gene (encoding the ortholog of mammalian MAP1LC3A) was also modulated by both Gs in zebrafish cells along with 2 other genes corresponding to proteins of the family of mammalian orthologs of yeast Atg8, (Gabarap and Gabarapl2/Gate-16 in zebrafish). These 3 proteins are involved in the elongation of the autophasome membrane in mammals.[30] Other authors[17,34-37] give a more comprehensive and detailed account of the functions and roles of these proteins in autophagy.

Type I IFN-mediated response induced by rhabdoviral Gs is regulated by autophagy in zebrafish cells

Once confirmed that rhabdoviral G proteins can modulate autophagy in vivo, we wondered whether or not a relationship exists between autophagy modulation and the immune response elicited by these proteins, such as the activation of the type I IFN system. To that end, cells were transfected with the rhabdoviral G-encoding plasmids in the presence or absence of autophagy chemical modulators (3MA and rapamycin) and 48 h post-transfection the expression of interferon stimulated gene *mx* (isoforms A and B) was evaluated. As a positive control of activation of this type I IFN response, poly (I:C)-treated cells were included in the assay. The *mx* gene was chosen because Mx proteins have
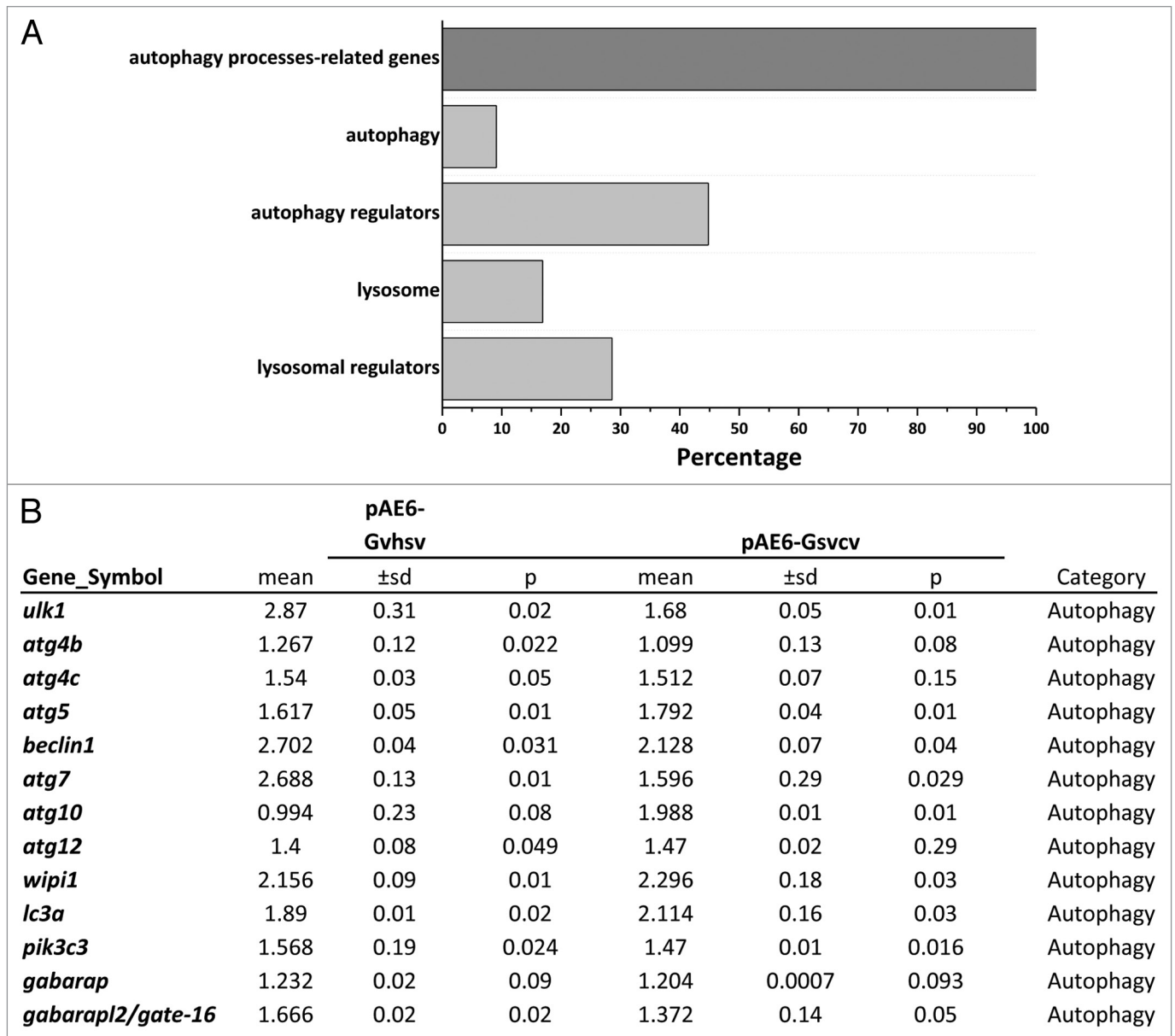
Figure 4. Expression of genes related to autophagy by microarray hybridization obtained from adult zebrafish genetically immunized by intramuscular injection with pAE6, pAE6-Gvhsv, or pAE6-Gsvcv. Three d post-immunization, muscle samples of zebrafish intramuscularly injected with 1.5 µg of the plasmids were processed to obtain their gene expression profiles using commercially available whole-genome DNA oligo microarrays from Agilent. Autophagy-related genes differentially expressed were sub-categorized (**A**). The expression fold values of the genes in the sub-category *autophagy*, are tabulated (**B**). Gene expression values were calculated by normalizing them against pAE6-injected fish. Means and standard deviations (S.D.) were calculated from 3 independent experiments. Threshold for statistical significance was established at $P \leq 0.05$.

The table in panel B:

Gene_Symbol	pAE6-Gvhsv mean	±sd	p	pAE6-Gsvcv mean	±sd	p	Category
ulk1	2.87	0.31	0.02	1.68	0.05	0.01	Autophagy
atg4b	1.267	0.12	0.022	1.099	0.13	0.08	Autophagy
atg4c	1.54	0.03	0.05	1.512	0.07	0.15	Autophagy
atg5	1.617	0.05	0.01	1.792	0.04	0.01	Autophagy
beclin1	2.702	0.04	0.031	2.128	0.07	0.04	Autophagy
atg7	2.688	0.13	0.01	1.596	0.29	0.029	Autophagy
atg10	0.994	0.23	0.08	1.988	0.01	0.01	Autophagy
atg12	1.4	0.08	0.049	1.47	0.02	0.29	Autophagy
wipi1	2.156	0.09	0.01	2.296	0.18	0.03	Autophagy
lc3a	1.89	0.01	0.02	2.114	0.16	0.03	Autophagy
pik3c3	1.568	0.19	0.024	1.47	0.01	0.016	Autophagy
gabarap	1.232	0.02	0.09	1.204	0.0007	0.093	Autophagy
gabarapl2/gate-16	1.666	0.02	0.02	1.372	0.14	0.05	Autophagy

proven to be very specific and sensitive markers for type I IFN responses.[38,39]

In the absence of autophagy chemical modulators, the 3 viral glycoproteins, Gsvcv, Gvhsv, and Gvsv, were able to significantly upregulate the transcript expression of *mx* genes by 6-, 3-, and 2.9-fold, respectively, compared with untransfected cells (**Fig. 5**). Likewise, *mx* gene expression was also induced in cells treated with poly (I:C). In contrast, no upregulation of *mx* transcripts was observed in cells transfected with plasmids coding for the TFP protein alone (**Fig. 5**). In all 3 cases,

3MA reduced ≥ 50% the *mx* gene expression (**Fig. 5**). Conversely, rapamycin induced an increase of 50% the *mx* expression in G-expressing cells. As expected, neither 3MA nor rapamycin had significant effects on the *mx* expression in cells transfected with the plasmid encoding TFP alone when compared with untransfected cells. Overall, these results suggest that i) autophagy is required for the activation of the type I IFN response by rhabdoviral Gs and ii) there is a synergistic effect of rapamycin and rhabdovrial Gs on type I IFN activation.
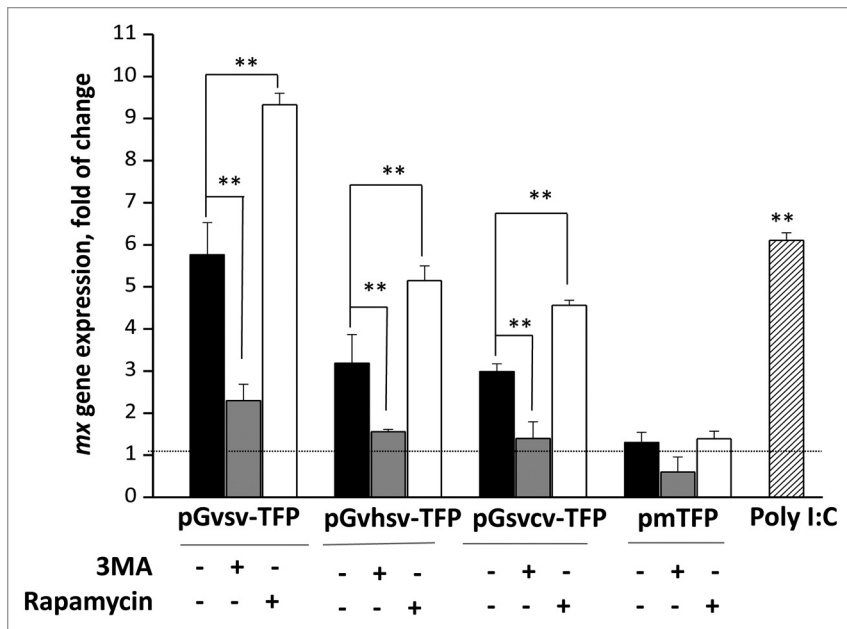
Figure 5. Modulation of *mx* mediated by G-induced autophagy. ZF4 cells were transfected with 0.5 µg/mL of pGvsv-TFP, pGvhsv-TFP, pGsvcv-TFP, or pmTFP. Four hours post-transfection, the media were removed and replaced by fresh cell culture media or media containing 10 mM of 3MA or 500 nM of rapamycin. Media were renewed after 24 h. At 48 h cells were harvested for RNA isolation and the transcript abundance of *mx* was analyzed by RTqPCR and calculated with the $2^{-\Delta\Delta Ct}$ method, using *eef1a1l1* (eukaryotic translation elongation factor 1 α, like 1) as endogenous control. Bars represent the mean expression ± SD of 2 independent experiments. **Statistically significant ($P \le 0.05$). Dotted line, expression levels of untransfected control cells.

Identification of the major autophagy-inducing regions of the Gs of VSV and VHSV

It has been reported that specific autophagy-inducing agents such as the Tat–BECN1 peptide may have potential for the prevention and treatment of a broad range of human diseases.[40] In this context, we wondered if specific regions of rhabdoviral Gs might suffice to initiate the antiviral autophagy response. If that were the case, the identification of these protein regions/peptides could be of crucial interest for the development of antiviral agents at least these rhabdoviruses. With the aim of identifying these potential G autophagy-inducing regions sets of 15-mer overlapping peptides (pepscan) spanning the entire sequence of the G corresponding to VHSV (07.71 serotype), and VSV (Indiana strain) were synthesized. Between the SVCV and VHSV we chose VHSV because abundant data on its G sequence and structure is available.[41] To carry out the assays, cells grown in 24-well plates were treated with each of the 15-mer synthetic peptides from the pepscan of Gvsv (HaCaT cells) or Gvhsv (ZF4 cells) and the induction of autophagy was evaluated by flow cytometry using an anti-LC3 protein antibody.

Three of the 43 peptides from the Gvsv pepscan induced a significant increase of autophagy in peptide-treated HaCaT cells relative to untreated cells (**Fig. 6A**; **Fig. S5A**). These 3 autophagy-inducing peptides defined 2 separated regions located at the fusion and lateral domains of the protein according to

the prefusion structure of Gvsv.[42] The region located at the fusion domain (from amino acid 77 to 91) (**Fig. 6A**, blue) was defined by one peptide (p84, **Table 1**), which increased the LC3 protein-associated fluorescence by »3-fold. The second region (from amino acid 337 to 361) (**Fig. 6A**, red) was defined by the pepscan peptides p344 and p354 (**Table 1**), which increased the LC3 protein-associated fluorescence by ≈6.5- and 3.5-fold, respectively (**Fig. 6A**).

Interestingly, an autophagy-inducing peptide (from amino acid 99 to 113) (**Fig. 6B**, blue) in the fusion domain (p106, **Table 1**) was also identified in the sequence of Gvhsv (**Fig. 6B**; **Fig. S5B**). These results suggest a pivotal role of the fusion domain of rhabdoviral Gs in autophagy activation. In fact, the p106 peptide was previously described as one of most important phosphatidylserine (PS)-binding peptide of Gvhsv.[44] In contrast, no peptides implicated in the autophagy activation were found in other domains of Gvhsv.

To confirm the role in autophagy of the G inducing-peptides, mapped by pepscan, the presence of the lipidated form of LC3 (LC3-II), as analyzed by WB (**Fig. 6C and D**), was investigated in cells treated with those peptides. In the case of Gvhsv, we also included in the study the p2 peptide (amino acids [aa] 83 to 109 of Gvhsv) which overlaps with p106 and can bind not only PS but also phosphatidylinositol bisphosphate.[45] Since phosphatidylinositol plays an important role in autophagy processes,[46,47] it was interesting to test whether or not p2 was also implicated in triggering autophagy.

In agreement with the FC data, cell treatment with the above-mentioned Gvsv or Gvhsv autophagy-inducing peptides resulted in autophagy induction, as demonstrated by an increment of the conversion of LC3-I to LC3-II, compared with untreated cells or cells treated with a noninducing peptide (Np) (**Fig. 6C and D**). Thus, the LC3-II/LC3-I ratios in mammalian cells treated with Gvsv autophagy-inducing peptides were 2.29, 4.63, and 2.78 for the peptides p84, p344, and 354, respectively (**Fig. 6C**), which, in FC assays, increased the LC3 fluorescence 3-, 6.5-, and 3.5-fold compared with untreated cells (**Fig. 6A**). For Gvhsv autophagy-inducing peptides the LC3-II/LC3-I ratios were 5.08 and 7.01 for p106 and p2, respectively (**Fig. 6D**). All these results suggest a relationship between Gvhsv PS- and PtdIns-binding regions and autophagosome formation.

Major autophagy-inducing peptides of the Gs of VSV and VHSV inhibit viral replication

If autophagy plays an antiviral role during rhabdovirus infection and one of the viral PAMPs that activates the antiviral autophagy is the G, we hypothesized that cell treatment with the major rhabdoviral autophagy-inducing peptides should decrease viral replication. To check this hypothesis, cells were treated with each of the autophagy-inducing peptides of VHSV or VSV Gs.
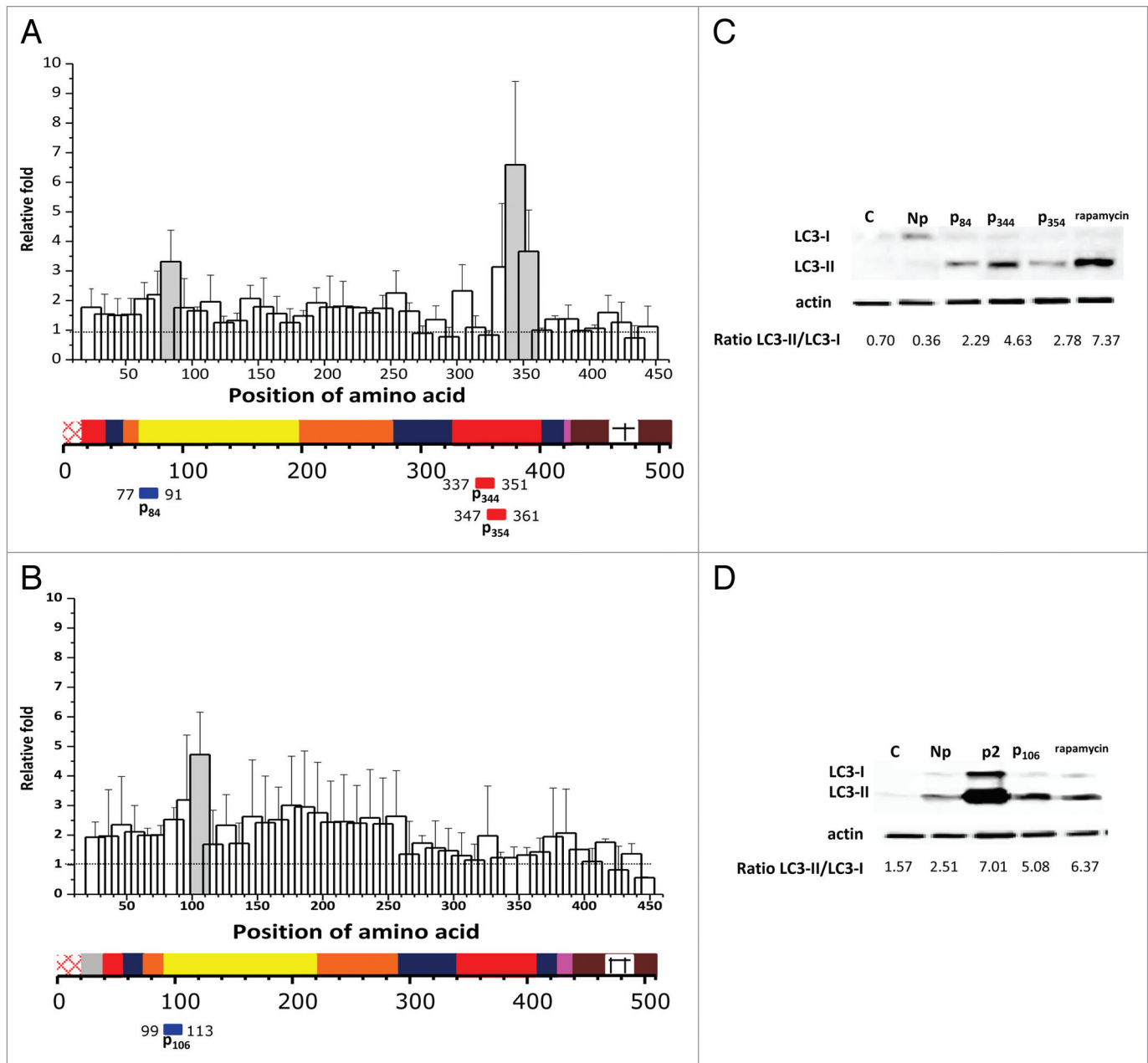
Figure 6. Relative fold changes in LC3 protein expression in response to VSV and VHSV G pepscan peptide assayed by flow cytometry and immunoblot analysis of selected peptides. (**A and B**) Cells grown in 24-well plates, were incubated with 25 μg/mL of each of the peptides from the Gvsv and Gvhsv pepscans of 15-mer peptides. After 24 h of incubation, LC3 protein expression was measured by flow cytometry using an anti-LC3 antibody. Fold increases were calculated relative to untreated cells. Data represented are the mean fold ± SD from 2 independent experiments, each performed in duplicate. Grey bars represent pepscan peptides that induced significant changes in LC3 protein expression at $P \leq 0.05$. Dotted lines indicate expression levels of untreated cells. Sequences of Gvsv and Gvhsv are represented colored by domains.[41-43] Signal peptide (red checkerboard), DI (lateral domain, red); DII (trimerization domain, blue); DIII (PH domain, orange); DIV (fusion domain, yellow); Cter (Cterminal, magenta); unobserved Cter (brown), with TM (black checkerboard). (**C and D**) Representative blots of ZF4 and HaCaT cells treated with the selected G peptides from VSV (P84, P344, P354) and VHSV (P106) and p2 (Gvhsv PS- and phosphatidylinositol bisphosphate-binding peptide). Cells were treated with 25 μg/mL of the peptides for 24 h, rapamycin (positive control), and a negative control peptide (Np), as a negative control. The transferred proteins were stained with anti-LC3 antibody. LC3-II/LC3-I ratios were calculated by densitometry and their values indicated below the blots.

Twenty-four hours after treatment, cells were washed and then infected with SVCV or VHSV (multiplicity of infection [moi] 0.1) and the amount of newly synthesized virus particles released into the cell media evaluated. Those VHSV (p106) and VSV (p84, p344 and p354) G autophagy-inducing peptides showing higher LC3-II/LC3-I ratios (**Fig. 6C and D**) displayed a significant antiviral activity.

On the one hand, at the maximum concentration used (50 μg/ml), the autophagy-inducing peptides belonging the fusion domains of both Gs (Gvsv and Gvhsv) reduced the SVCV

Table 1. Sequence and position of the pepscan peptides in the sequence of Gvhsv and Gvsv

Gvhsv		Gvsv	
Pepscan peptide no.[a]	Sequence to C terminus	Pepscan peptide no.	Sequence to C terminus
26	TPQITQRPPVENIST	24	KFTIVFPHNQKGNWK
36	ENISTYHADWDTPLY	34	KGNWKNVPSNYHYCP
46	DTPLYTHPSNCRDDS	44	YHYCPSSSDLNWHND
56	CRDDSFVPIRPAQLR	54	NWHNDLIGTGLQVKM
66	PAQLRCPHEFEDINK	64	LQVKMPKSHKAIQAD
76	EDINKGLVSVPTRII	74	AIQADGWMCHASKWV
86	PTRIIHLPLSVTSVS	84	ASKWVTTCDFRWYGP
96	VTSVSAVASGHYLHR	94	RWYGPKYITHSIRSF
106	HYLHRVTYRVTCSTS	104	SIRSFTPSVEQCKES
116	TCSTSFFGGQTIEKT	114	QCKESIEQTKQGTWL
126	TIEKTILEAKLSRQE	124	QGTWLNPGFPPQSCG
136	LSRQEATDEASKDHE	134	PQSCGYATVTDAEAV
146	SKDHEYPFFPEPSCI	144	DAEAVIVQVTPHHVL
156	EPSCIWMKNNVHKDI	154	PHHVLVDEYTGEWVD
166	VHKDITHYYKTPKTV	164	GEWVDSQFINGKCSN
176	TPKTVSVDLYSRKFL	174	GKCSNDICPTVHNST
186	SRKFLNPDFIEGVCT	184	VHNSTTWHSDYKVKG
196	EGVCTTSPCQTHWQG	194	YKVKGLCDSNLISTD
206	THWQGVYWVGATPKA	204	LISTDITFFSEDREL
216	ATPKAHCPTSETLEG	214	EDRELSSLGKEGTGF
226	ETLEGHLFIRTHDHR	224	EGTGFRSNYFAYETG
236	THDHRVVKAIVAGHH	234	AYETGDKACKMQYCK
246	VAGHHPWGLTMACTV	244	MQYCKHWGVRLPSGV
256	MACTVTFCGTEWIKT	254	LPSGVWFEMADKDLF
266	EWIKTDLGDLIQVTG	264	DKDLFAAARFPECPE
276	IQVTGPGGTRKLTPN	274	PECPEGSSISAPSQT
286	KLTPNKCVNTDIQMR	284	APSQTSVDVSLIQDV
296	DIQMRGATDDFSYLN	294	LIQDVERILDYSLCQ
306	FSYLNHLITNMAQRT	304	YSLCQETWSKIRAGL
316	MAQRTECLDAHSDIT	314	IRAGLPISPVDLSYL
326	HSDITASGKVSSFLL	324	DLSYLAPKNPGTGPA
336	SSFLLSKFRPSHPGP	334	GTGPAFTIINGTLKY
346	SHPGPGKAHYLLDGQ	344	GTLKYFETRYIRVDI
356	LLDGQIMRGDCDYEA	354	IRVDIAAPILSRMVG
366	CDYEAVVSINYNRAQ	364	SRMVGMISGTTTERE
376	YNRAQYKTMNNTWKS	374	TTERELWDDWAPYED
386	NTWKSWKRVDNNTDG	384	APYEDVEIGPNGVLR
396	NNTDGYDGMIFGDKL	394	NGVLRTSSGYKFPLY
406	FGDKLIIPDIEKYQS	404	KFPLYMIGHGMLDSG
416	EKYQSVYDSGMLVQR	414	MLDSGLHLSSKAQVF
426	MLVQRNLVEVPHLSI	424	KAQVFEHPHIQDAAS
436	PHLSIVFVSNTSDLS	434	QDAASQLPDDEILFF
446	TSDLSTNHIHTNLIP	444	EILFFGDTGLSKNPI

[a]The peptides were named by the N-terminal position of their middle amino acid (8th position) in their protein sequence.

or VHSV titers ~10-fold in ZF4 cells, (**Fig. 7A and B**). Furthermore, the Gvhsv p2 peptide, which also exhibited a high LC3-II/LC3-I ratio expression, reduced the viral yields of VHSV and SVCV infections ~10-fold at the lowest concentration used (**Fig. 7A and B**). On the other hand, 50μg/ml of Gvsv autophagy-inducing peptides, located toward the C-terminal of the protein (p344 and p354), also reduced the VHSV and SVCV titers ~10-fold in ZF4 cells. Curiously, these peptides were more effective against VHSV (**Fig. 7A**) than SVCV (**Fig. 7B**), even though VSV and SVCV are phylogenetically closer to each other.[48]

It is noteworthy that regardless of the source of the autophagy-inducing peptides (Gvsv or Gvhsv), protection against any of the 2 viruses was achieved. Thus, the decrease of the viral titers probably reflects xenophagic degradation of the viruses. Alternatively, this may also be due to other antiviral effects, which result from increased autophagy.

Discussion

The lysosomal degradation pathway of autophagy has a crucial role in the defense against some viral infections.[10] Accordingly, agents capable of modulating autophagy may have broad therapeutic applications.[5] One approach to developing such agents is to exploit autophagy-manipulation strategies used by microbial virulence factors[40] while another approach might use viral mechanisms. To that end, in this work we have studied the relationship between the surface antigen (the glycoptoyein G) of 3 viruses belonging to the *Rhabdoviridae* family (VSV, VHSV, and SVCV) and autophagy. As a result, we identified functionally relevant short regions of the rhabdoviral Gs that induce autophagy and reduce virus propagation. These regions might be used for developing therapeutic applications.

First, our results showed that the activation of a cell antiviral autophagy upon infection might be a feature common to all rhabdoviruses regardless of the virus target host. In fact, fish rhabdoviruses, for which a relationship with autophagy had not been established previously, present a similar autophagy-related profile as that displayed by the mammalian rhabdovirus VSV in both vertebrate cell lines used in this work (ZF4 and HaCaT) and in insects cells previously used.[14,15]

Next, we demonstrated both in vitro (cell transfection assays) and in vivo (genetic immunization of adult zebrafish) that the G of rhabdoviruses is the PAMP that triggers antiviral autophagy. Moreover, under our experimental conditions

(transitory expression assays), cells expressing Gs for several days did not show signs of decreased viability (data not shown) in accordance with previous studies in which no loss of viability is reported in both mammalian and fish cell lines stably expressing rhabdoviral Gs.[41,49,50]

Furthermore, the inhibition of autophagy impaired the immune response induced by these proteins suggests that autophagy, most likely, is involved in the orchestration of the host immune response to these viral antigens. Similarly, ongoing autophagy is needed for VSV genome ((-) ssRNA) detection and IFNA secretion by plasmacytoid dendritic cells.[9]

In order to answer the question of how to exploit the rhabdoviral Gs ability to induce autophagy for the possible prevention and control of rhabdovirus infections, our strategy was to test the viral protein sequences to find those regions that trigger autophagy in cell culture. To that end, a pepscan of 15-mer overlapping peptides spanning the whole sequence of Gvsv and Gvhsv were synthesized and tested. As a result, peptides that significantly induced autophagy and reduced viral infection were identified. Strikingly, some of the autophagy-inducing peptides were located in the fusion domain of both VSV and VHSV Gs. Likewise, induction of autophagy in HIV-1 infected cell cultures was also triggered by the fusogenic activity of gp41,[51] the fusion protein of this virus. In the case of rhabdoviruses, the fusion domain should not be exposed on the G surface in the prefusion conformation since the viral-cell membrane fusion takes places in the endosomes.[52] Therefore, the ability of the rhabdoviral peptides located at the fusion domain of the G to induce autophagy suggests the potential presence of pattern recognition receptors leading to the activation of the autophagy signaling cascade(s) not only on the cell surface but also in the endosomes. Regarding VHSV G, the presence in its sequence of linear determinants that activate the type I IFN system has been reported (VHSV G Mx-inducing peptides).[41] In silico studies showed that these VHSV G Mx-inducing peptides were exposed on the surface of the protein. In contrast, autophagy-inducing peptides identified in this work are located in the fusion domain of the protein and therefore are only exposed during membrane fusion. Taken together, these results suggest that VHSV G glycoprotein might signal the IFN induction by means of its prefusion conformation (native conformation) and autophagy by means of its post-fusion conformation. However, more work is needed to confirm this hypothesis.
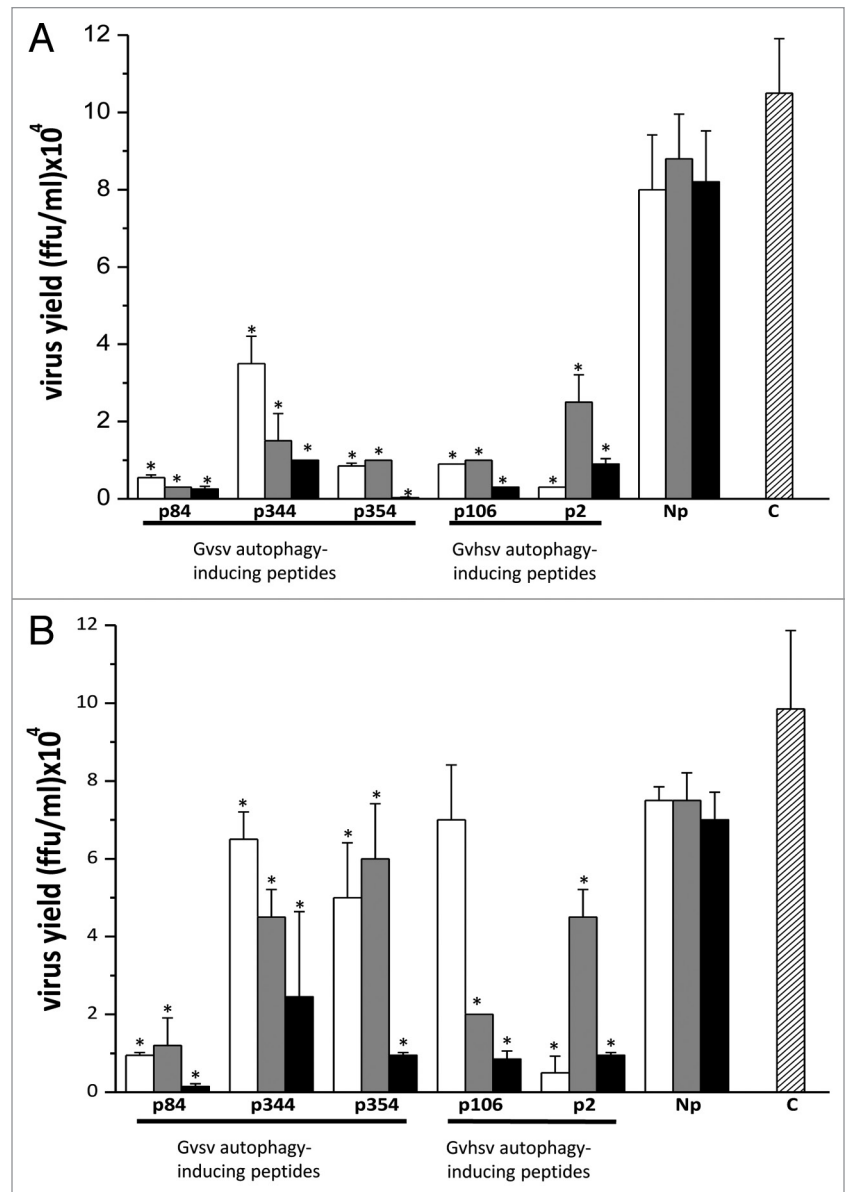
Despite the potential of the peptides identified in this work as autophagy modulators, it is not yet clear that their represented regions play the same role as part of the G molecule during rhabdoviral infection. Nevertheless, since these peptides upregulate autophagy and influence the outcome of rhabdoviral infections, G glycoproteins should be the target of future studies oriented at the modulation of autophagy for therapeutic purposes.

Figure 7. Antiviral effect of autophagy-inducing peptides in ZF4 cells. Titration of virus (in ffu/mL) recovered from cell culture media from ZF4 cells treated with 12 (white bars), 25 (gray bars) and 50 (black bars) μg/mL of autophagy-inducing peptides from VSV or VHSV Gs, a negative peptide (Np) or untreated and then infected with VHSV (**A**) or SVCV (**B**). The results represent the mean ± SD of 2 independent experiments each performed in duplicate. *, Statistically significant ($P \leq 0.05$), peptide treated vs. untreated cells.

Materials and Methods

Cell lines and viruses

The fish cell lines ZF4 (zebrafish embryonic fibroblast)[53] and EPC (*Epithelioma Papulosum Cyprini*)[54] cells, both purchased

from the American Type Culture Collection (ATCC, #CRL-2050 and CRL-2872, respectively), were used in this work. Cells were maintained at 28 °C in a 5% CO_2 atmosphere in RPMI-1640 Dutch modified (Gibco, 22409-015) cell culture medium containing 10% fetal bovine serum (FBS) (Sigma, F6178), 1 mM pyruvate (Gibco, 11360-039), 2 mM L-glutamine (Gibco, 25030-024), 50 μg/mL gentamicin (Gibco, 15750-060) and 2 μg/mL fungizone (Gibco, 15290-026). The human cell line HaCaT was purchased from CLS Cell Lines Service GmbH (Eppelheim, CLS order #300493). HaCaT cells were cultured in high glucose DMEM medium (Sigma, D5671) supplemented with 2 mM L-glutamine, 10% FBS, 1 mM pyruvate, 2 mM glutamine, 50 μg/mL gentamicin and 2 μg/mL fungizone, at 37 °C in a humidified incubator in a 5% CO_2 atmosphere.

The SVCV isolate 56/70, isolated from carp,[55] was propagated in ZF4 cells at 22 °C. VHSV (strain 07.71), isolated in France from rainbow trout (*Oncorhynchus mykiss*),[56] was propagated in EPC cells at 14 °C modified from Basurco et al.[57] Supernatants from VHSV- or SVCV-infected cell monolayers were clarified by centrifugation at 4,000 × g for 30 min and kept in aliquots at −80 °C. Clarified supernatants were used for the experiments. For the generation of nonreplicative SVCV and VHSV both viruses were UV-inactivated by 2 exposures to 1 J/cm² as described for VSV inactivation[9] using a Bio-Link Crosslinker BLX E312 (Vilber Lourmat, BLX-E312). Neither of the viruses could replicate after UV-irradiation (data not shown).

Antibodies

For visualization in immunofluorescence (IF), flow cytometry (FC), and protein staining in western blot (WB) assays of human and zebrafish microtubule-associated protein 1 light chain-3 (LC3)-I/LC3-II, a polyclonal antibody anti-LC3A/B (Cell Signaling Technology, 4108) was diluted 200- (IF) 300- (FC) and 1,000-fold (WB). IF assays and focus-forming assays of infection with VHSV and SVCV were performed using the monoclonal antibody 2C9[58,59] (against the N protein of VHSV, VHSV-N) and BIO 331 (against SVCV-N, BioX Diagnostics, BIO 331) diluted 1,000- and 300-fold, respectively. A monoclonal antibody anti-actin (Sigma, A2066) was used to stain human and zebrafish actin diluted 2,000-fold in WB assays. Goat anti-rabbit (GAR) CF™594 (Sigma, SAB4600107) fluorophore-conjugated antibody diluted 500-fold was used in IF assays. GAR CF™488 (Sigma, SAB4600389) fluorophore-conjugated antibody diluted 200-fold was used for autophagy activation/inhibition assays of the Pepscan peptides by FC. Goat anti-rabbit peroxidase-conjugated antibody (GAR-Po, Sigma, A6154) diluted 500-fold was used in WB assays for visualization of the LC3 band. Rabbit anti-mouse peroxidase-conjugated (RAM-Po, Sigma, A9044) diluted 300-fold was used in focus forming assays for both SVCV and VHSV.

Viral infectivity assays

ZF4 cells, grown in 96-well plates, were infected with VHSV or SVCV in a final volume of 100 μl/well of culture medium supplemented with 2% FBS for 90 min at 14 °C or 22 °C, respectively. Cells were then washed to remove unbound virus and culture media replaced with fresh RPMI 2% FBS. To test the effect of 3MA (Sigma, M9281) upon VHSV and SVCV infectivity, cell monolayers were treated with 3MA in DMSO (Sigma, 472301)/EtOH (1:1)[11] diluted 1/100 in cell culture medium to final concentration of 10 mM for 4 h before infection. In this case, a 0.05% of DMSO was added to the cell culture medium in every condition assayed.

To test the effect of the pepscan peptides upon VHSV and SVCV infectivity, cell monolayers were treated with different peptide concentrations for 24 h prior to infection. In all cases, after the incubation periods untreated or treated cells were washed extensively with phosphate-buffered saline (PBS; 100 mM Na_2HPO_4, 27 mM KCl, 17 mM KH_2PO_4, 1.3 M NaCl, pH 7.4) and infected with VHSV or SVCV as indicated above. At 24 h postinfection the supernatant fractions from infected cell cultures were harvested and the virus yields assayed by an immunostaining focus assay as described below.

Viral replication assays

SVCV and VHSV replication were determined by a previously described immunostaining focus assay.[60,61] EPC cells were incubated in 96-well plates with serial dilutions of the virus-containing supernatant fractions at either 14 °C (VHSV) or 22 °C (SVCV) for 24 h. Then, media were removed and cells fixed with a solution of 4% formaldehyde (Sigma, F1635) in PBS for 15 min. Cells were then washed with PBS and fixed with cold methanol (-20 °C) for 15 min, washed again with PBS and then incubated with the antibodies 2C9 (VHSV) or BIO 331 (SVCV) in dilution buffer [0.24 mM merthiolate (Sigma, T5125), 5 g of Tween-20 (Merck, 655204)/liter, and 50 mg of phenol red (Sigma, P3532)/liter in PBS, pH 6.8]. After incubation with primary antibodies cell monolayers were washed 3 times with distilled water and incubated with RAM-Po secondary antibody for 45 min and then washed 3 times with distilled water. Finally, 50 μl of 1 mg/mL of diaminobenzidine (DAB, Sigma, D5637) in PBS containing H_2O_2[58,61] was added to each well, and the reaction was allowed to proceed until brown foci were detected with an inverted microscope (Nikon). Brown foci were then counted to determine virus titers in focus forming units (ffu)/mL.

DNA plasmids

The cDNA sequences derived from the mRNAs encoding the membrane surface glycoproteins of SVCV (Gsvcv, GenBank accession Z37505.1) and VHSV (Gvhsv, GenBank accession A10182.1) were synthesized by GenScript USA Inc. The synthetic sequences were subcloned into pAE6, a plasmid containing the 5′-regulatory sequences of the gene encoding carp actb/β-actin,[20,62] following standard procedures to generate the plasmid constructs pAE6-Gsvcv and pAE6-Gvhsv, respectively. The same cDNA sequences were subcloned into the plasmid vector pmTFP (Allele Biotechnology, ABP-FP-TCNCS) containing the gene sequence of TFP)[18] to obtain the DNA constructs pGsvcv-TFP and pGvshv-TFP used in the in vitro experiments. The pmTFP plasmid contains the sequence of the human cytomegalovirus transcription promoter, a bacterial origin of replication for plasmid production, the simian virus 40 (SV40) polyA signal, and the ampicillin resistance gene sequence. For the experiments with the fusion protein containing the G of VSV, the construct pmTFP-VSV-G (Allele Biotechnology, ABP-FP-TVSVG10), hereafter referred to as pGvsv-TFP, was used.

Cell transfection assays

Cell transfection assays were performed as previously described.[63,64] Briefly, ZF4 cell monolayers, grown in culture flasks of 75 cm^2, were detached using Tryple Select (Gibco, 12563-029), washed, resuspended in cell culture medium supplemented with 10% FBS and dispensed into 24- or 96-well cell culture plates. The following day, plasmid DNA was incubated with 0.3 μl of FuGene 6 (Promega, E2691)/100 ng of pDNA for 30 min in RPMI-1640 without FBS. The mixes were then added (1/5 of the total volume of the culture medium in each well) to the wells containing the cells. Plasmid DNA concentrations, temperatures, and times are indicated for each experiment. In HaCaT, cells transfection mixes (0.3 μl of FuGene 6/250 ng of pmTFP or pGvsv-TFP plasmid) were performed using DMEM cell culture medium and added to cells in suspension. Then cells were seeded and incubated at 37 °C for the times indicated in each experiment.

Immunofluorescence assays

Untreated-, transfected-, or infected-cell monolayers were fixed with a 4% formaldehyde solution in PBS for 15 min at room temperature (RT). After washing the fixed cells, plates were further fixed with cold methanol (-20 °C) for 15 min. Cell monolayers were then incubated overnight at 4 °C with the anti-LC3 antibody in dilution buffer (PBS with 0.03% Triton X 100 [Sigma, T8787]) and 5% of albumin from bovine serum (BSA, Sigma, A2153). After that, monolayers were washed again and incubated with GAR CF™594 (in dilution buffer) for 1 h to visualize LC3. Finally, cells were washed and stained with 1 μg/mL of 4′-6-Diamidino-2-phenylindole (DAPI) for 10 min. Cell monolayers were then viewed and photographed with an inverted fluorescence microscope (Nikon Eclipse TE2000-U; Nikon Instruments, Inc., NY) provided with a digital camera (Nikon DS-1QM, Nikon Instruments, Inc., NY).

Fusion assays

To assess the functionality of the G ectodomain of the G-TFP fusion proteins encoded in the plasmids, ZF4 cells were transfected in 96-well plates as indicated above with 0.5 μg/mL of pGsvcv-TFP, pGvhsv-TFP, or pGvsv-TFP. After 3 d, cell culture media were removed, cells were washed and cell membrane fusion was triggered by incubating the cells with fusion medium[60] at pH 6 for 30 min. Media were then removed and cell monolayers were washed and subsequently incubated at room temperature with fusion medium at pH 7.5 for 2 h. Finally, cells were fixed with a 4% formaldehyde solution (in PBS) for 15 min and then with cold methanol (–20 °C) for 15 min. Cell nuclei were stained with DAPI (1 μg/mL) for 10 min and washed again with PBS. Cell monolayers were then viewed and photographed with an inverted fluorescence microscope provided with a digital camera.

In vitro gene expression assays by reverse transcriptase quantitative polymerase chain reaction (RTqPCR)

The transcript expression levels of the interferon-stimulated gene (ISG) *mx* (both isoforms A and B) were evaluated in ZF4 cells at 48 h post-transfection with G-TFP-encoding plasmids in the presence or absence of 3MA (10 mM) or rapamycin (500 nM; Sigma, R8781). Cells treated with 40 μg/mL of polyinosine polycytidylic acid (poly (I:C), P1038, Sigma) for 18 h were used as a positive control of *mx* induction. After the different incubation time periods, the medium was removed, and cells processed for total RNA extraction as indicated below. The *mx* levels were evaluated by RTqPCR using specific primers (**Table S1**) and SYBR green (as indicated below). The *mx* induction assays results were analyzed by using the $2^{-\Delta\Delta Ct}$ method,[65] and the *eef1a1l1* gene as endogenous control. Control cells (untransfected and untreated cells) served as calibrator and folds were calculated by the formula transfected cells/untransfected cells.

Zebrafish

Adult zebrafish (*Danio rerio*) of 2 to 3 g (≈4 cm in length) were obtained from a local pet shop and maintained at 28 °C in 30 l tanks equipped with a re-circulating dechlorinated water system. Fish were fed daily with a commercial feed diet. Prior to experiments, fish were acclimatized to laboratory conditions for at least 2 wk. All experiments with live animals (zebrafish) were performed using protocols approved by the European Union Council Guidelines (86/609/EU).

Genetic immunization of zebrafish with pAE6-G plasmids

Adult zebrafish were intramuscularly injected (n = 4) with 10 μl of a solution containing 1.5 μg of pAE6-Gsvcv, pAE6-Gvhsv or pAE6 in PBS. Prior to injections, zebrafish were anesthetized by immersion in 50 μg/mL buffered tricaine methanesulfonate (MS-222; Sigma, E10521). Three d post-injection muscle samples were excised from the injection site and total RNA extracted as indicated below. First, G expression was analyzed by RTqPCR using specific primers and probes for VHSV and SVCV Gs (**Table S1**) and calculated with the $2^{-\Delta Ct}$ method using the *eef1a1l1* as endogenous control as mentioned above. Next, RNA samples were used for microarray assays.

RNA isolation

The E.Z.N.A HP Total RNA kit (Omega bio-tek, R6812) and E.Z.N.A HP Tissue RNA kit (Omega bio-tek, R6688), for the in vitro and the in vivo experiments, respectively, were used for total RNA extraction in accordance with instructions provided by the manufacturer. Isolated RNAs were stored at –80 °C until used. For the microarray gene expression experiments, RNA samples were grouped into pools of 4 muscle samples from 4 different zebrafish for each treatment.

cDNA synthesis and RT-qPCR assays

For the in vivo G expression assays individual muscle samples were used. One microgram of RNA, as estimated by a NanoDrop® Spectrophotometer (Nanodrop Technologies, Wilmington, DE, USA) was used to obtain the cDNA using the Moloney murine leukemia virus reverse transcriptase (M-MLV, Invitrogen, 28025-013) as previously described.[66] Quantitative PCR was then performed using the ABI PRISM 7,300 System (Applied Biosystems NY, USA) as previously described.[41] Primers and probes used in both in vitro and in vivo expression assays are listed in **Table S1**. Reactions were performed in a total volume of 20 μl comprising 2 μl of cDNA reaction mixture, 900 nM of each primer, 10 μl of TaqMan universal PCR master mix (Applied Biosystems, 4304437) with 200 nM of probe or 10 μl of SYBR green PCR master mix (Applied Biosystems, 4309155). The cycling conditions were 50 °C for 2 min and 95 °C for 10 min, followed by 40 cycles at 95 °C for 15 s and

60 °C for 1 min. Nontemplate controls (NTCs) and controls without reverse transcriptase were included for each gene in all RT-qPCR assays (data not shown).

RNA labeling and microarray hybridization

Microarray hybridizations were performed using the ZEBRAFISH v. Two (ID 026437) 4 × 44 K Agilent oligonucleotide microarray using single-color labeling. Standard methods were used for all processes according to manufacturer's instructions (Agilent Technologies). Briefly, each amplified and labeled sample was hybridized at 65 °C for 17 h. Microarrays were scanned and one-channel TIFF images (FEATURE EXTRACTION software v. 10.4.0.0) were imported into GENESPRING software (GX v.11.0) for preliminary analysis. Microarray data described in accordance with MIAME guidelines was submitted to the Gene Expression Omnibus (GEO) database (no. GSE49626).

Normalizations were performed by correcting the individual probe fluorescence in each microarray with the sum of all the fluorescent values according to the formula, fluorescence of each probe/sum of all of the probe fluorescences per microarray. After normalization, outlier values (defined by those fluorescence values > or < mean ± standard deviation per probe) were identified and eliminated (masked) from the calculations programmed in Origin pro 8.6 (OriginLab Corporation, Northampton, MA USA). Comparisons with the pAE6 plasmid were calculated for each probe by using the following formula, fluorescent value from zebrafish injected with pAE6-Gvhsv or pAE6-Gsvcv plasmids/mean fluorescent value from zebrafish injected with pAE6 (n = 4). Means and standard deviations of the folds were then calculated (n = 4). A double simultaneous criterion to define differentially expressed gene transcripts was used: i) genes with folds > 1.5 or < 0.66 and ii) genes with folds deviated from the null hypothesis at $P < 0.05$.

Classification of zebrafish genes in autophagy-lysosomal related pathways

A list of human gene symbols classified as participants in autophagy and autophagy related-processes[25] were used to search for those genes related to authophagy present in the zebrafish microarray. The zebrafish orthologs (of genes in the list mentioned above), autophagy-related gene symbols and their associated folds, standard deviations, and P values were extracted from the microarray data by using a macro in Excel (Microsoft Corporation).

Pepscans derived from the sequences of the glycoproteins G (Gs) of VSV and VHSV

The synthesis of the 15-mer peptides with an overlap of 5 amino acids (aa) and spanning the cDNA-derived aa sequence of the VHSV07.71 G[67] and VSV G[68] (GenBank accession numbers A10182 and X03633, respectively) was performed by Mimotopes Pty Ltd. The pepscan peptides (**Table 1**) were named by a number corresponding to the position of their middle aa (8th position) in their corresponding G. The Peptide p2 (from aa 82 to 109 of VHSV G (IIHLPLSVTSVSAVASGHYLHRVTYRVT) was synthesized by Clontech. Peptides were diluted in water to a final concentration of 2 mg/mL.

Evaluation of the autophagy induced by VHSV and VSV G peptides by flow cytometry (FC)

ZF4 and HaCaT cells grown in 24-well plates were treated with 25 μg/mL of each of the VHSV and VSV G pepscan peptides, respectively, for 24 h (at 28 °C for ZF4 cells and 37 °C for HaCaT cells). In all cases, after the incubation the expression of the LC3 protein was quantified by FC following methologies previously described.[69] Briefly, peptide-treated cell monolayers were permeabilized with 0.05% saponin (Sigma, S4521) and incubated with anti-LC3 antibody diluted 200-fold in FACS buffer consisting of PBS (100 mM Na_2HPO_4, 27 mM KCl, 17 mM KH_2PO_4, 1.3 M NaCl, pH 7.4), 0.05% saponin and goat serum (Sigma, G6767) for 1 h at RT. After washing, cell monolayers were incubated with GAR CF488A-conjugated secondary antibody diluted 200-fold with FACS buffer for 30 min at RT. After washing, cell monolayers were detached and fixed with 1% paraformaldehyde. The expression of LC3 was analyzed with a BD FACS Canto™ II flow cytometer (BD Biosciences) using the FACSDiva v6.3.1 (Becton Dickinson) software. For each sample 10,000 cells (events) were analyzed. The total fluorescence in the selected gate for each peptide was calculated by multiplying the mean fluorescence intensity by their event count. To compare different experiments, the results of each experiment were normalized by the mean fluorescence of all the peptides and expressed as relative to untreated cells (fluorescence of peptide-treated cells/fluorescence of control cells). The results are the means and standard deviations from 2 different independent experiments each performed in duplicate.

In vitro cell viability assays

To exclude nonspecific effects of the autophagy regulators (3MA and rapamycin) due to cellular toxicity, cell viability was quantified by using an MTT (3-(4,5-Dimethyl-2-thiazolyl)-2,5-diphenyl-2H-tetrazolium bromide) Cell Titer 96 Non-Radioactive Cell Proliferation Assay (Promega, G109A) following the manufacturer instructions. Cytotoxicity was assayed 48 h after ZF4 or HaCaT cell monolayers were exposed to different concentrations of 3MA (2 to 12 mM) or rapamycin (200 to 600 nM).

Western blot assays

ZF4 or HaCaT cells were grown on 24-well plates in culture medium supplemented with 10% FBS at 28 °C or 37 °C, respectively. After 24 h, the different treatments (3MA, rapamycin, pepscan peptides, or plasmids) were added. Once the treatments were finished, culture media were removed and cell monolayers were resuspended in 500 μl of PBS with a cocktail of protease inhibitors (Sigma, P8340). Cells were then frozen/thawed 4 times and protein concentration adjusted before loading protein samples onto the gel. Samples were loaded in Tris–Glycine sodium dodecyl sulfate 15% polyacrylamide gels under reducing conditions. Electrophoresis was performed at 100 V for 90 min. For blotting, the proteins in the gel were transferred for 75 min at 100 V in transfer buffer (2.5 mM Tris, 9 mM glycine, 20% methanol) to nitrocellulose membranes (BioRad, 162-0115). The membranes were then blocked with 8% dry milk, 0.05% Tween-20 in PBS and incubated with primary antibodies in PBS containing 5% BSA and 0.1% Tween-20 as indicated by the manufacturer. Membranes were then washed 3 times with PBS containing 0.05% Tween-20 for 15 min before incubation

with GAR-Po in 0.5% milk in PBS for 90 min. Finally, the membrane was washed 3 times with PBS containing 0.05% Tween-20 and the peroxidase activity was detected by using ECL chemiluminescence reagents (Amersham Biosciences, RPN2232) and revealed by exposure to X-ray. Protein bands were analyzed by densitometry using the Scion Image 4.0.2 Software (www.scionorg.com). Analysis of LC3-I and LC3-II bands was performed and calculated as relative to the actin intensity band. Results are presented as the ratio of LC3-II/LC3-I.

Statistical analysis

Statistical analysis was performed using the Graph Pad Prism 5 (GraphPad software, Inc.). All data are shown as means ± standard deviations (SD). Differences were evaluated using a 2-tailed independent Student t test. Statistical differences were considered significant when $P \leq 0.05$ (**) or $P < 0.01$ (***).

References

1. Levine B, Klionsky DJ. Development by self-digestion: molecular mechanisms and biological functions of autophagy. Dev Cell 2004; 6:463-77; PMID:15068787; http://dx.doi.org/10.1016/S1534-5807(04)00099-1

2. Ravikumar B, Futter M, Jahreiss L, Korolchuk VI, Lichtenberg M, Luo S, Massey DC, Menzies FM, Narayanan U, Renna M, et al. Mammalian macroautophagy at a glance. J Cell Sci 2009; 122:1707-11; PMID:19461070; http://dx.doi.org/10.1242/jcs.031773

3. Choi AM, Ryter SW, Levine B. Autophagy in human health and disease. N Engl J Med 2013; 368:651-62; PMID:23406030; http://dx.doi.org/10.1056/NEJMra1205406

4. Klionsky DJ, Baehrecke EH, Brumell JH, Chu CT, Codogno P, Cuervo AM, et al. A comprehensive glossary of autophagy-related molecules and processes (2nd edition). Autophagy 2011; 7:1273-94.

5. Tovilovic G, Ristic B, Milenkovic M, Stanojevic M, Trajkovic V. The role and therapeutic potential of autophagy modulation in controlling virus-induced cell death. Med Res Rev 2014; 34:744-67; PMID:24123125; http://dx.doi.org/10.1002/med.21303

6. Dales S, Eggers HJ, Tamm I, Palade GE. Electron Microscopic Study of the Formation of Poliovirus. Virology 1965; 26:379-89; PMID:14319710; http://dx.doi.org/10.1016/0042-6822(65)90001-2

7. Shoji-Kawata S, Levine B. Autophagy, antiviral immunity, and viral countermeasures. Biochim Biophys Acta 2009; 1793:1478-84; PMID:19264100; http://dx.doi.org/10.1016/j.bbamcr.2009.02.008

8. Dreux M, Chisari FV. Viruses and the autophagy machinery. Cell Cycle 2010; 9:1295-307; PMID:20305376; http://dx.doi.org/10.4161/cc.9.7.11109

9. Lee HK, Lund JM, Ramanathan B, Mizushima N, Iwasaki A. Autophagy-dependent viral recognition by plasmacytoid dendritic cells. Science 2007; 315:1398-401; PMID:17272685; http://dx.doi.org/10.1126/science.1136880

10. Dong X, Levine B. Autophagy and viruses: adversaries or allies? J Innate Immun 2013; 5:480-93; PMID:23391695; http://dx.doi.org/10.1159/000346388

11. Jackson WT, Giddings TH Jr., Taylor MP, Mulinyawe S, Rabinovitch M, Kopito RR, Kirkegaard K. Subversion of cellular autophagosomal machinery by RNA viruses. PLoS Biol 2005; 3:e156; PMID:15884975; http://dx.doi.org/10.1371/journal.pbio.0030156

12. Heaton NS, Randall G. Dengue virus and autophagy. Viruses 2011; 3:1332-41; PMID:21994782; http://dx.doi.org/10.3390/v3081332

13. Lee YR, Hu HY, Kuo SH, Lei HY, Lin YS, Yeh TM, Liu CC, Liu HS. Dengue virus infection induces autophagy: an in vivo study. J Biomed Sci 2013; 20:65; PMID:24011333; http://dx.doi.org/10.1186/1423-0127-20-65

14. Shelly S, Lukinova N, Bambina S, Berman A, Cherry S. Autophagy is an essential component of Drosophila immunity against vesicular stomatitis virus. Immunity 2009; 30:588-98; PMID:19362021; http://dx.doi.org/10.1016/j.immuni.2009.02.009

15. Cherry S. VSV infection is sensed by Drosophila, attenuates nutrient signaling, and thereby activates antiviral autophagy. Autophagy 2009; 5:1062-3; PMID:19713743; http://dx.doi.org/10.4161/auto.5.7.9730

16. Nakamoto M, Moy RH, Xu J, Bambina S, Yasunaga A, Shelly SS, Gold B, Cherry S. Virus recognition by Toll-7 activates antiviral autophagy in Drosophila. Immunity 2012; 36:658-67; PMID:22464169; http://dx.doi.org/10.1016/j.immuni.2012.03.003

17. Levine B, Mizushima N, Virgin HW. Autophagy in immunity and inflammation. Nature 2011; 469:323-35; PMID:21248839; http://dx.doi.org/10.1038/nature09782

18. Ai HW, Olenych SG, Wong P, Davidson MW, Campbell RE. Hue-shifted monomeric variants of Clavularia cyan fluorescent protein: identification of the molecular determinants of color and applications in fluorescence imaging. BMC Biol 2008; 6:13; PMID:18325109; http://dx.doi.org/10.1186/1741-7007-6-13

19. Klionsky DJ, Abeliovich H, Agostinis P, Agrawal DK, Aliev G, Askew DS, Baba M, Baehrecke EH, Bahr BA, Ballabio A, et al. Guidelines for the use and interpretation of assays for monitoring autophagy in higher eukaryotes. Autophagy 2008; 4:151-75; PMID:18188003

20. Chico V, Ortega-Villaizan M, Falco A, Tafalla C, Perez L, Coll JM, Estepa A. The immunogenicity of viral haemorrhagic septicaemia rhabdovirus (VHSV) DNA vaccines can depend on plasmid regulatory sequences. Vaccine 2009; 27:1938-48; PMID:19368775; http://dx.doi.org/10.1016/j.vaccine.2009.01.103

21. Lorenzen N, Lorenzen E, Einer-Jensen K, LaPatra SE. DNA vaccines as a tool for analysing the protective immune response against rhabdoviruses in rainbow trout. Fish Shellfish Immunol 2002; 12:439-53; PMID:12194454; http://dx.doi.org/10.1006/fsim.2002.0422

22. Emmenegger EJ, Kurath G. DNA vaccine protects ornamental koi (Cyprinus carpio koi) against North American spring viremia of carp virus. Vaccine 2008; 26:6415-21; PMID:18812203; http://dx.doi.org/10.1016/j.vaccine.2008.08.071

23. García-Valtanen P, Martinez-Lopez A, Ortega-Villaizan M, Perez L, Coll JM, Estepa A. In addition to its antiviral and immunomodulatory properties, the zebrafish β-defensin 2 (zfBD2) is a potent viral DNA vaccine molecular adjuvant. Antiviral Res 2014; 101:136-47; PMID:24286781; http://dx.doi.org/10.1016/j.antiviral.2013.11.009

24. Xiang ZQ, Spitalnik SL, Cheng J, Erikson J, Wojczyk B, Ertl HC. Immune responses to nucleic acid vaccines to rabies virus. Virology 1995; 209:569-79; PMID:7778289; http://dx.doi.org/10.1006/viro.1995.1289

25. Jegga AG, Schneider L, Ouyang X, Zhang J. Systems biology of the autophagy-lysosomal pathway. Autophagy 2011; 7:477-89; PMID:21293178; http://dx.doi.org/10.4161/auto.7.5.14811

26. Cheong H, Nair U, Geng J, Klionsky DJ. The Atg1 kinase complex is involved in the regulation of protein recruitment to initiate sequestering vesicle formation for nonspecific autophagy in Saccharomyces cerevisiae. Mol Biol Cell 2008; 19:668-81; PMID:18077553; http://dx.doi.org/10.1091/mbc.E07-08-0826

27. Itakura E, Mizushima N. Characterization of autophagosome formation site by a hierarchical analysis of mammalian Atg proteins. Autophagy 2010; 6:764-76; PMID:20639694; http://dx.doi.org/10.4161/auto.6.6.12709

28. Kabeya Y, Kamada Y, Baba M, Takikawa H, Sasaki M, Ohsumi Y. Atg17 functions in cooperation with Atg1 and Atg13 in yeast autophagy. Mol Biol Cell 2005; 16:2544-53; PMID:15743910; http://dx.doi.org/10.1091/mbc.E04-08-0669

29. Kamada Y, Funakoshi T, Shintani T, Nagano K, Ohsumi M, Ohsumi Y. Tor-mediated induction of autophagy via an Apg1 protein kinase complex. J Cell Biol 2000; 150:1507-13; PMID:10995454; http://dx.doi.org/10.1083/jcb.150.6.1507

30. Kabeya Y, Mizushima N, Yamamoto A, Oshitani-Okamoto S, Ohsumi Y, Yoshimori T. LC3, GABARAP and GATE16 localize to autophagosomal membrane depending on form-II formation. J Cell Sci 2004; 117:2805-12; PMID:15169837; http://dx.doi.org/10.1242/jcs.01131

31. Kirisako T, Ichimura Y, Okada H, Kabeya Y, Mizushima N, Yoshimori T, Ohsumi M, Takao T, Noda T, Ohsumi Y. The reversible modification regulates the membrane-binding state of Apg8/Aut7 essential for autophagy and the cytoplasm to vacuole targeting pathway. J Cell Biol 2000; 151:263-76; PMID:11038174; http://dx.doi.org/10.1083/jcb.151.2.263

32. Mizushima N, Yoshimori T, Ohsumi Y. The role of Atg proteins in autophagosome formation. Annu Rev Cell Dev Biol 2011; 27:107-32; PMID:21801009; http://dx.doi.org/10.1146/annurev-cellbio-092910-154005

33. Mauthe M, Yu W, Krut O, Krönke M, Götz F, Robenek H, Proikas-Cezanne T. WIPI-1 Positive Autophagosome-Like Vesicles Entrap Pathogenic Staphylococcus aureus for Lysosomal Degradation. Int J Cell Biol 2012; 2012:179207; PMID:22829830; http://dx.doi.org/10.1155/2012/179207

34. Deretic V, Levine B. Autophagy, immunity, and microbial adaptations. Cell Host Microbe 2009; 5:527-49; PMID:19527881; http://dx.doi.org/10.1016/j.chom.2009.05.016

35. Kang R, Zeh HJ, Lotze MT, Tang D. The Beclin 1 network regulates autophagy and apoptosis. Cell Death Differ 2011; 18:571-80; PMID:21311563; http://dx.doi.org/10.1038/cdd.2010.191

36. Mizushima N, Levine B. Autophagy in mammalian development and differentiation. Nat Cell Biol 2010; 12:823-30; PMID:20811354; http://dx.doi.org/10.1038/ncb0910-823

37. Lamb CA, Dooley HC, Tooze SA. Endocytosis and autophagy: Shared machinery for degradation. Bioessays 2013; 35:34-45; PMID:23147242; http://dx.doi.org/10.1002/bies.201200130

38. von Wussow P, Jakschies D, Hochkeppel HK, Fibich C, Penner L, Deicher H. The human intracellular Mx-homologous protein is specifically induced by type I interferons. Eur J Immunol 1990; 20:2015-9; PMID:2120071; http://dx.doi.org/10.1002/eji.1830200920

39. Simon A, Fäh J, Haller O, Staeheli P. Interferon-regulated Mx genes are not responsive to interleukin-1, tumor necrosis factor, and other cytokines. J Virol 1991; 65:968-71; PMID:1702845

40. Shoji-Kawata S, Sumpter R, Leveno M, Campbell GR, Zou Z, Kinch L, Wilkins AD, Sun Q, Pallauf K, MacDuff D, et al. Identification of a candidate therapeutic autophagy-inducing peptide. Nature 2013; 494:201-6; PMID:23364696; http://dx.doi.org/10.1038/nature11866

41. Chico V, Martinez-Lopez A, Ortega-Villaizan M, Falco A, Perez L, Coll JM, Estepa A. Pepscan mapping of viral hemorrhagic septicemia virus glycoprotein G major lineal determinants implicated in triggering host cell antiviral responses mediated by type I interferon. J Virol 2010; 84:7140-50; PMID:20463070; http://dx.doi.org/10.1128/JVI.00023-10

42. Roche S, Rey FA, Gaudin Y, Bressanelli S. Structure of the prefusion form of the vesicular stomatitis virus glycoprotein G. Science 2007; 315:843-8; PMID:17289996; http://dx.doi.org/10.1126/science.1135710

43. Roche S, Bressanelli S, Rey FA, Gaudin Y. Crystal structure of the low-pH form of the vesicular stomatitis virus glycoprotein G. Science 2006; 313:187-91; PMID:16840692; http://dx.doi.org/10.1126/science.1127683

44. Estepa A, Coll JM. Pepscan mapping and fusion-related properties of the major phosphatidylserine-binding domain of the glycoprotein of viral hemorrhagic septicemia virus, a salmonid rhabdovirus. Virology 1996; 216:60-70; PMID:8615007; http://dx.doi.org/10.1006/viro.1996.0034

45. Estepa AM, Rocha AI, Mas V, Pérez L, Encinar JA, Nuñez E, Fernandez A, Gonzalez Ros JM, Gavilanes F, Coll JM. A protein G fragment from the salmonid viral hemorrhagic septicemia rhabdovirus induces cell-to-cell fusion and membrane phosphatidylserine translocation at low pH. J Biol Chem 2001; 276:46268-75; PMID:11590161; http://dx.doi.org/10.1074/jbc.M108682200

46. Criollo A, Maiuri MC, Tasdemir E, Vitale I, Fiebig AA, Andrews D, Molgó J, Díaz J, Lavandero S, Harper F, et al. Regulation of autophagy by the inositol trisphosphate receptor. Cell Death Differ 2007; 14:1029-39; PMID:17256008

47. Criollo A, Vicencio JM, Tasdemir E, Maiuri MC, Lavandero S, Kroemer G. The inositol trisphosphate receptor in the control of autophagy. Autophagy 2007; 3:350-3; PMID:17404493

48. Kurath G. Molecular Epidemiology and Evolution of Fish Novirhabdoviruses. in Rhabdoviruses: Molecular Taxonomy, Evolution, Genomics, Ecology, Host-Vector Interactions, Cytopathology and Control chapter 7 2012:pp.89-116. Caister Academic Press

49. Burger SR, Remaley AT, Danley JM, Moore J, Muschel RJ, Wunner WH, Spitalnik SL. Stable expression of rabies virus glycoprotein in Chinese hamster ovary cells. J Gen Virol 1991; 72:359-67; PMID:1993876; http://dx.doi.org/10.1099/0022-1317-72-2-359

50. Florkiewicz RZ, Smith A, Bergmann JE, Rose JK. Isolation of stable mouse cell lines that express cell surface and secreted forms of the vesicular stomatitis virus glycoprotein. J Cell Biol 1983; 97:1381-8; PMID:6415065; http://dx.doi.org/10.1083/jcb.97.5.1381

51. Denizot M, Varbanov M, Espert L, Robert-Hebmann V, Sagnier S, Garcia E, Curriu M, Mamoun R, Blanco J, Biard-Piechaczyk M. HIV-1 gp41 fusogenic function triggers autophagy in uninfected cells. Autophagy 2008; 4:998-1008; PMID:18818518

52. Albertini AA, Baquero E, Ferlin A, Gaudin Y. Molecular and cellular aspects of rhabdovirus entry. Viruses 2012; 4:117-39; PMID:22355455; http://dx.doi.org/10.3390/v4010117

53. Driever W, Rangini Z. Characterization of a cell line derived from zebrafish (Brachydanio rerio) embryos. In Vitro Cell Dev Biol Anim 1993; 29A:749-54; PMID:8407719; http://dx.doi.org/10.1007/BF02631432

54. Winton J, Batts W, deKinkelin P, LeBerre M, Bremont M, Fijan N. Current lineages of the epithelioma papulosum cyprini (EPC) cell line are contaminated with fathead minnow, Pimephales promelas, cells. J Fish Dis 2010; 33:701-4; PMID:20497291; http://dx.doi.org/10.1111/j.1365-2761.2010.01165.x

55. Stone DM, Ahne W, Denham KL, Dixon PF, Liu CT, Sheppard AM, Taylor GR, Way K. Nucleotide sequence analysis of the glycoprotein gene of putative spring viraemia of carp virus and pike fry rhabdovirus isolates reveals four genogroups. Dis Aquat Organ 2003; 53:203-10; PMID:12691191; http://dx.doi.org/10.3354/dao053203

56. DeKinkelin P, Geraed JP, Dorson M, Le Berre M. Viral Haemorrhagic Septicemia: Demostration of a protective immune response following natural infection. Fish Health News 1977; 6:43-5

57. Basurco B, Coll JM. Spanish isolates and reference strains of viral haemorrhagic septicaemia virus shown similar protein size patterns. Bull Eur Assoc Fish Pathol 1989; 9:92-5

58. Sanz F, Coll JM. Detection of viral haemorrhagic septicemia virus by direct immunoperoxidase with selected anti-nucleoprotein monoclonal antibody. Bull Eur Assoc Fish Pathol 1992; 12:116-9

59. Mas V, Rocha A, Perez L, Coll JM, Estepa A. Reversible inhibition of spreading of in vitro infection and imbalance of viral protein accumulation at low pH in viral hemorrhagic septicemia rhabdovirus, a salmonid rhabdovirus. J Virol 2004; 78:1936-44; PMID:14747558; http://dx.doi.org/10.1128/JVI.78.4.1936-1944.2004

60. Mas V, Pérez L, Encinar JA, Pastor MT, Rocha A, Perez-Paya E, Ferrer-Montiel A, Gonzalez Ros JM, Estepa A, Coll JM. Salmonid viral haemorrhagic septicaemia virus: fusion-related enhancement of virus infectivity by peptides derived from viral glycoprotein G or a combinatorial library. J Gen Virol 2002; 83:2671-81; PMID:12388802

61. Lorenzo G, Estepa A, Coll JM. Fast neutralization/immunoperoxidase assay for viral haemorrhagic septicaemia with anti-nucleoprotein monoclonal antibody. J Virol Methods 1996; 58:1-6; PMID:8783145; http://dx.doi.org/10.1016/0166-0934(95)01972-3

62. Brocal I, Falco A, Mas V, Rocha A, Perez L, Coll JM, Estepa A. Stable expression of bioactive recombinant pleurocidin in a fish cell line. Appl Microbiol Biotechnol 2006; 72:1217-28; PMID:16636829; http://dx.doi.org/10.1007/s00253-006-0393-7

63. Lopez A, Fernandez-Alonso M, Rocha A, Estepa A, Coll JM. Transfection of epithelioma cyprini (EPC) carp cells. Biotechnol Lett 2001; 23:481-7; http://dx.doi.org/10.1023/A:1010393723002

64. Ortega-Villaizan M, Chico V, Martinez-Lopez A, Falco A, Perez L, Coll JM, Estepa A. In vitro analysis of the factors contributing to the antiviral state induced by a plasmid encoding the viral haemorrhagic septicaemia virus glycoprotein G in transfected trout cells. Vaccine 2011; 29:737-43; PMID:21095250; http://dx.doi.org/10.1016/j.vaccine.2010.11.021

65. Livak KJ, Schmittgen TD. Analysis of relative gene expression data using real-time quantitative PCR and the 2(-Delta Delta C(T)) Method. Methods 2001; 25:402-8; PMID:11846609; http://dx.doi.org/10.1006/meth.2001.1262

66. Falco A, Chico V, Marroquí L, Perez L, Coll JM, Estepa A. Expression and antiviral activity of a beta-defensin-like peptide identified in the rainbow trout (Oncorhynchus mykiss) EST sequences. Mol Immunol 2008; 45:757-65; PMID:17692376; http://dx.doi.org/10.1016/j.molimm.2007.06.358

67. Thiry M, Lecocq-Xhonneux F, Dheur I, Renard A, de Kinkelin P. Molecular cloning of the mRNA coding for the G protein of the viral haemorrhagic septicaemia (VHS) of salmonids. Vet Microbiol 1990; 23:221-6; PMID:2402872; http://dx.doi.org/10.1016/0378-1135(90)90152-L

68. Vandepol SB, Lefrancois L, Holland JJ. Sequences of the major antibody binding epitopes of the Indiana serotype of vesicular stomatitis virus. Virology 1986; 148:312-25; PMID:2417417; http://dx.doi.org/10.1016/0042-6822(86)90328-4

69. Eng KE, Panas MD, Karlsson Hedestam GB, McInerney GM. A novel quantitative flow cytometry-based assay for autophagy. Autophagy 2010; 6:634-41; PMID:20458170; http://dx.doi.org/10.4161/auto.6.5.12112